Soc. Am. **67**, 1 (1977).
14. H. Kanamori and K. Satake, *Geophys. Res. Lett.* **17**, 1179 (1990).
15. The data for Fig. 3 have been passed through a median filter to enhance coherent features. A median filter is similar to the more familiar running mean filter, except that the median, rather than the mean, is used. Use of a median filter is preferred for time series with a large number of isolated outliers, which is the case for the geyser data. This filter preserves the sharpness of step-like changes in a time series. The sample length in Fig. 3 is 20 samples corresponding to between 15 and 30 hours. See W. H. Press, B. P. Flannery, S. A. Teukolsky, W. T. Vetterling, *Numerical Recipes* (Cambridge Univ. Press, Cambridge, 1986).
16. J. Rinehart, *Geysers and Geothermal Energy* (Springer-Verlag, New York, 1980).
17. S. W. Kieffer, *J. Volcanol. Geotherm. Res.* **22**, 59 (1984).
18. S. W. Kieffer, *Rev. Geophys.* **27**, 3 (1989).
19. D. Brock, personal communication.
20. The formula given is for the probability of exactly two interval-lengthening events and one mode-changing event being coincident with an earthquake, although the number quoted is for at least this number of coincidences.
21. The probability is most sensitive to the estimates of $N_{g\ell}$ and N_{gm}. It is unlikely, however, that we have underestimated these values by more than about 30%, which would increase the probability by no more than a factor of 3. One could argue that, for the preseismic case, it is more appropriate to consider N_e to be 5 rather than 3, on the basis of the number of events with comparable static strain (Fig. 2). Using this value increases P by a factor of 5. Allowing for both of these factors increases in probability, $P \sim 0.014$, which is still below the critical value for significance, taken here to be 0.05.
22. M. T. Gladwin, R. L. Gwyther, R. Hart, M. Francis, M. J. S. Johnston, *J. Geophys. Res.* **92**, 7981 (1987).
23. K. Mogi, *Earthquake Prediction* (Academic Press, Tokyo, 1985).
24. A. C. Fraser-Smith *et al.*, *Geophys. Res. Lett.* **17**, 1465 (1990).
25. V. I. Keilis-Borok, L. Knopoff, I. M. Rotwain, C. R. Allen, *Nature* **335**, 690 (1988).
26. S. Rojstaczer, *Eos* **72**, 121 (1991).
27. C. R. Carrigan, G. C. P. King, G. E. Barr, N. E. Bixler, *Geology* **19**, 1157 (1991).
28. A. Nur, personal communication.
29. We thank O. Kolbek and the other workers at Calistoga Geyser, whose diligent monitoring of the geyser has made this study possible. We thank D. Power, who along with J. Dunlap and A. Sawyer entered more than 150,000 eruption times into the computer. E. Roeloffs, P. Rydelek, G. Helffrich, A. Linde, and I. Cifuentes provided reviews. We also thank A. Linde for numerous stimulating conversations as well as S. Sacks, S. Kieffer, D. White, S. Rojstaczer, S. Hickman, J. Rinehart, C. Carrigan, and D. Brock for helpful discussions. We thank M. Johnston for providing strain data. We thank M. Acierno for computer support and J. Dunlap for assistance with manuscript preparation. This research was sponsored by the Department of Terrestrial Magnetism, Carnegie Institution of Washington.

RESEARCH ARTICLE

Short-Lived Radioactivity and Magma Genesis

James Gill and Michel Condomines

Short-lived decay products of uranium and thorium have half-lives and chemistries sensitive to the processes and time scales of magma genesis, including partial melting in the mantle and magmatic differentiation in the crust. Radioactive disequilibrium between ^{238}U, ^{230}Th, and ^{226}Ra is widespread in volcanic rocks. These disequilibria and the isotopic composition of thorium depend especially on the extent and rate of melting as well as the presence and composition of vapor during melting. The duration of mantle melting may be several hundred millennia, whereas ascent times are a few decades to thousands of years. Differentiation of most magmas commonly occurs within a few millennia, but felsic ones can be tens of millennia old upon eruption.

Magmas form as the result of decompression of the mantle, advection of heat, or fluxing by fluids such as water. They originate by partial melting at grain boundaries and drain upward by permeable flow, eventually ascending in sheets or pipes. Afterward they evolve chemically (differentiate) when they stall, often in reservoirs in or near the base of the crust, through the precipitation of minerals (fractional crystallization) and exsolution of vapor in a closed system or through open-system processes such as mixing with other magmas or chemical exchange with the reservoir's surroundings (assimilation). We refer to these two processes as melting and differentiation, respectively, although in practice they may not be as separate in space or time as we implied above. Together they span the "age of magma," that is, the time between the beginning of partial melting and the eruption of this melt or its differentiate.

The types of magma as well as their processes and rates of formation vary in different tectonic settings. Buoyancy is primarily responsible for the separation of basaltic melt from matrix beneath large intraplate volcanoes such as Hawaii, whereas shear stress is more important at plate margin volcanoes at spreading centers and subduction zones (*1*). Some magmas must ascend through the crust at rates of a few centimeters per second, because they transport dense mantle xenoliths to the surface, whereas others have characteristics attributed to prolonged crustal interaction. Radioactive disequilibria are used to study three aspects of magma genesis: (i) the melting process, (ii) ascent and differentiation, and (iii) the source materials. We focus on ^{238}U-^{230}Th-^{226}Ra disequilibria and the ^{230}Th/^{232}Th tracer in volcanic rocks that have erupted during the last few millennia (*2–4*).

In addition to providing the heat that fuels convection and partial melting, the natural radioactive decays of U and Th produce short-lived nuclides that may provide quantitative measurements of trace element fractionation and porosity and of constraints on the temporal and spatial scale of magma formation. There are 41 intermediate decay products in the three U and Th decay chains, seven of which have been studied in magmatic systems (Table 1). These products and their parents include actinides (Th, U, Pa), an alkaline earth (Ra), a rare gas (Rn), and chalcophilic elements of low and variable volatility (Pb, Bi, Po). In addition, the behavior of U during magma genesis is sensitive to its oxidation state and fluid composition because its solubility in magmatic fluids increases with O fugacity (f_{O_2}) and the concentration of Cl or CO_3^{2-} in the fluids.

This topic is usually known as the study of U series disequilibrium (*5*). Secular radioactive equilibrium is reached when the numbers of atoms (N) of all nuclides in a decay series are inversely proportional to their decay constants (λ) so that their "activities" (λ^*N) are equal. Equilibrium is reached after about five half-lives of the longest lived nuclide. Both melting and differentiation involve chemical reactions between solids, silicate or carbonate melts, and vapor composed of C, H, O, and halogens. These reactions fractionate many elements including those in the ^{238}U-^{206}Pb, ^{235}U-^{207}Pb, and ^{232}Th-^{208}Pb decay chains, resulting in disequilibrium (unequal activities) between nuclides in one or more of the decay series (Fig. 1). Trace element fractionations have long been used in the study of magma genesis processes. However, because radioactive equilibrium exists at the beginning of magma formation and is re-

---

J. Gill is with the Earth Sciences Department, University of California, Santa Cruz, CA. M. Condomines is at the Centre de Recherches Volcanologiques et URA 10 CNRS, Université Blaise Pascal, 63038 Clermont-Ferrand, France.

gained at known rates afterward, these particular fractionations constrain rates and independently quantify processes.

In addition, the isotopic composition of Th (the $^{230}Th/^{232}Th$ ratio) is sensitive to the time scale of melting and ascent and to small differences in source composition. Thorium's isotope ratios respond quickly to changes in source composition, making it the only isotopic tracer that reflects a current ratio of source trace elements (the Th/U ratio). In contrast, for example, Pb isotopes reflect the history of U/Pb and Th/Pb ratios of the source. The Th/U ratio that is inferred from Pb isotopes integrates that history, whereas Th isotopes measure the source's Th/U ratio at the time of melting. Other than He, Th and Ra are the most incompatible isotopic tracers in silicate melts and show the greatest variations, whereas tetravalent Th has the lowest solid-state diffusion coefficient (6). This combination gives Th the highest thermal Peclet number of the isotopic tracers, making it the least likely to reach chemical equilibrium during melting (*7*).

Several conventions are in use. Parentheses around a nuclide denote activities in disintegrations per minute per gram, whereas brackets denote concentrations in parts per million. The $(^{238}U)/(^{230}Th)$ activity ratio is referred to as k and the $(^{226}Ra)/(^{230}Th)$ activity ratio as ℓ. Thus, k or $\ell \neq 1.0$ indicates disequilibrium within the ^{238}U series; $k > 1.0$ indicates the presence of excess ^{238}U relative to ^{230}Th. From the decay constants in Table 1, $[U] = 1.350\ (^{238}U)$, $[Th] = 4.096\ (^{232}Th)$, a $(^{238}U)/(^{232}Th)$ ratio of 1.00 corresponds to a [Th/U] ratio of 3.034, and a $(^{230}Th)/(^{232}Th)$ ratio of 1.00 corresponds to a $[^{232}Th/^{230}Th]$ atomic ratio of 185,856.

Because activities change during magma formation, it is necessary to distinguish important stages of the process (Fig. 1). The $(^{230}Th)/(^{232}Th)$ ratio of the source at the start of melting is $(Th)_S$. Both $(^{230}Th)/(^{232}Th)$ and $(^{238}U)/(^{230}Th)$ ratios may rise during melting (during time t_0) so that by the end of the melting $(^{230}Th)/(^{232}Th)$ is $(Th)_0$ and $(^{238}U)/(^{230}Th)$ is k_0 (8). Such melts will then approach radioactive equilibrium through the decay of unsupported ^{230}Th. The $(^{230}Th)/(^{232}Th)$ ratio decays during ascent and differentiation (during time t_i); it is $(Th)_i$ at eruption, which is the "initial" Th isotope ratio of the rock. This decay continues during the time between eruption and measurement (t_m, the conventional age of the rock), resulting in $(Th)_m$ at the time of measurement.

The total time between initiation of melting and eruption (the age of magma) equals $t_0 + t_i$, intervals that are separated by the time at which chemical equilibrium between melt and source ends. At extremes, these intervals may correspond to the time of permeable flow of primitive melts through the asthenosphere versus ascent and differentiation in sheets or pipes through the lithosphere, respectively. However, a continuum in the porosity and spacing of melt channels is likely. Chemical equilibrium will be reached when channels are closely spaced and solid-state diffusion is rapid; chemical disequilibrium is enhanced by the opposite conditions and is likely even in the asthenosphere (*7*). If a source had been a closed chemical system for more than 350,000 years before partial melting and if $(t_0 + t_i)$ is less than 10,000 years, then $(Th)_i = (Th)_s = 3.034/[Th/U]_{source}$.

Historical Developments

The original motivation to study short-lived radioactivity in volcanic rocks was to date the rocks. Although analyses were made as early as 1905 by Joly, systematic work did not begin until the mid-1960s when a way was proposed to measure t_m (Fig. 2A) (9). Modern U-Th disequilibrium studies were developed during the 1970s (*10–12*) and blossomed during the 1980s (*3*). As of early 1992, analyses of Th-U nuclides had been published for about 500 samples from almost 150 volcanoes or mid-ocean ridge segments; data relating to ^{226}Ra are included for about 60% of these.

Alpha spectrometry was initially used for measurements of (^{234}U) and (^{230}Th) in igneous rocks, as in other applications of U-series disequilibria. This method requires long counting times, even when U and Th are purified from several grams of rock, because concentrations are usually low (0.01 to 5 ppm U, and 0.03 to 20 ppm Th). Chemical difficulties cause additional inaccuracy and irreproducibility, and the situation is worse for mineral separates. Consequently, practical limits of precision and accuracy are 2 to 5% at 2σ uncertainty.

In volcanic rocks (^{226}Ra) is less well established and is usually measured indirectly (*13–16*). Each of these methods can be precise to within 5% 2σ or better and can show (^{238}U)-(^{226}Ra) equilibrium in old samples, but some have calibration problems, and interlaboratory standardization has not been undertaken. Disequilibria >10% are considered reliable, although apparent excess ^{226}Ra measured indirectly with ^{210}Po in rocks <100 years old can reflect excess ^{210}Pb in accumulated feldspars rather than ^{226}Ra (*17*).

Table 1. Radionuclides used in igneous geochemistry. Half-lives in years except ^{210}Po, in days.

Actinides	Alkaline earths	Chalcophiles
^{232}Th	^{226}Ra	^{210}Pb
(1.401×10^{10})	(1600)	(22)
^{238}U	^{228}Ra	^{210}Po
(4.47×10^{9})	(5.77)	(138.4)
^{235}U		
(7.038×10^{8})		
^{234}U		
(2.47×10^{5})		
^{230}Th		
(7.54×10^{4})		
^{231}Pa		
(3.25×10^{4})		

The principal and most recent analytical development in this field is the precise measurement of small numbers of atoms and high atomic ratios with pulse-counting mass spectrometry. Thorium is the most important and difficult element in this respect. Accuracy to less than 1% in volcanic rocks requires measuring ^{230}Th intensities of 10^{-18} A, an abundance sensitivity of ≤ 0.2 ppm at mass 231 relative to 232, and reproducible measurement of isotope ratios with a dynamic range of 10^5 to 10^6. After a decade of effort, this accuracy has been achieved in several laboratories during the last 2 years. Several different types of mass spectrometers and analytical strategies have been used (*18–22*), most of which yield an improvement in standard error by a factor of 10 (0.25 to 0.5% 2σ) and a reduction in sample size by a factor of 2 or more compared to results obtained with alpha spectrometry. With several hundred nanograms of Th, $^{232}Th/^{230}Th$ ratios of ~350,000 have been measured with a 2σ uncertainty of 0.5% by thermal ionization mass spectrometry (*19*), and this small an uncertainty can be achieved with as little as a few tens of nanograms of Th by secondary ionization mass spectrometry (*21*). Calibration uncertainties so far limit the accuracy of $(^{230}Th)/(^{232}Th)$ ratios to about ±1%, but this too should improve soon by a factor of 2 or more. The radionuclides ^{234}U, ^{226}Ra, and ^{231}Pa also are being measured with mass spectrometry for volcanic rocks (*18–26*).

Melting Processes and Time Scales

Until recently, magma compositions were predominantly interpreted on the basis of batch partial melting models (*27*). The degree of melting was tacitly assumed to equal a melt fraction or porosity (ϕ) that could be calculated from the composition of undifferentiated basalts on the assumption that the final melt and the entire solid matrix were in chemical equilibrium. Elements that partition strongly into the melt (incompatible elements, with $D_i < 0.02$, where D_i is the partition coefficient, the concentration of element i in the bulk solid divided by its concentration in the melt) are most concentrated in small degree melts. Both the D's and the initial source composition must be known to calculate ϕ. Large differences in ϕ were identified for various magmas. Tholeiites, such as those that erupted at mid-ocean ridges or Hawaiian shield volcanoes, represented relatively large degrees of melting (10 to 20%), whereas alkali basalts reflected smaller percent melts (<5%), and highly alkalic magmas such as lamproites were smaller still.

Radioactive disequilibria allow for independent measurements of the degree of melting if a few partition coefficients are known and chemical equilibrium is reached. Initial radioactive equilibrium makes knowledge of the source composition unnecessary, and only the D's of parent and daughter nuclides are necessary in order to calculate ϕ. The ubiquity of radioactive disequilibria in lavas has encouraged rejection of batch melting models and raised hopes that the disequilibria can be used to quantify melt fractions and melting rates.

For example, both Th and U are highly incompatible [$D = 0.001$ to 0.01 (*6*)], and $D_U \sim D_{Th}$ was expected so that the [Th/U] ratio of melt would differ from that of source peridotite only in highly alkalic magmas. Discovery of an average 18% excess ^{230}Th ($k = 0.85$; $N = 50$) in mid-ocean ridge basalt (MORB) was, therefore, surprising (*11, 18, 28–30*). If related to melting, it implies that the mantle was permeable at low porosity and $D_{Th} < D_U$, so that Th was preferentially enriched at small degrees of melting, which are important even during MORB genesis. Continuous models that involve fractional melting (distillation) above a small ϕ, as well as dynamic models involving mixing of melts formed by small degrees of melting of variously depleted levels of an upwelling source, are required to reconcile the low k values with other geochemical results (*8, 31*).

Discovery of other, even larger disequilibria followed. Some MORB and island arc volcanic rocks have (^{226}Ra)/(^{230}Th) and (^{231}Pa)/(^{235}U) ratios of 1.5 to 3.0 (*2, 13, 15–18, 26, 29–30, 32–34*). Most of the excess ^{226}Ra in island arcs can be attributed to melting processes because it is present in primitive lavas and decreases in more differentiated ones of some volcanoes (Batur, Etna) and arcs (Eolian, Sangihe, and Papua New Guinea) (*15, 17, 32–35*). Enrichment of Ra is greater in MORBs and island arc basalts than in intraplate basalts, where it is usually <30% and commonly zero (*29, 36, 37*). The absence of large Ra excesses in intraplate volcanoes does not seem to reflect longer ascent times because some of the lavas that were analyzed are quite mafic and some of the volcanoes have high levels of historical activity (Kilauea, Reunion, Nyamuragira, and Mount Cameroon).

Radioactive disequilibria can constrain physical models of magma genesis. In current models it is assumed that there is chemical equilibrium between melt and major mantle minerals, and the principles are similar to those for dating ground water (*38*), although ^{234}U-^{238}U disequilibrium is usually absent in igneous rocks. The average migration time of nuclides in the flow direction can be calculated if the extent and rate of chemical interaction between fluid and matrix are specified. In the following example, we make the simplifying assumptions that variations in the [Th/U], (^{230}Th)/(^{232}Th), and k ratios reflect the degree and rate of melting rather than the source composition, and that there is chemical equilibrium between melt and mantle during melting but no interaction during ascent. The [Th/U] ratios and [Th] decrease with increasing degrees of partial melting until $[Th/U]_{melt}$ equals $[Th/U]_{source}$. This decrease is accompanied by an increase in (^{230}Th)/(^{232}Th) if the duration of melting (t_0) is longer than 100,000 years (8) and by a decrease in Th isotope ratios if the ascent time (t_i) is longer than 10,000 years (Fig. 1). The decrease in Th isotope ratios is accentuated if the products of small degrees of melting take millennia longer to reach the surface than do larger melt fractions.

Quantitative implications of disequilibria among Th, U, and Ra for melting have not yet been explored in detail because other trace element and isotopic measures of source homogeneity and percent of melting have not been available for the same samples. Some recent studies illustrate the potential for understanding melting processes, however. Along the Endeavor–Juan de Fuca spreading ridge in the northeast Pacific, k ratios vary inversely with Th contents and [Th/U] ratios for lavas that have similar Sr and Th isotope ratios (*18*). Between the southern Juan de Fuca and northern Gorda ridges, (^{230}Th)/(^{238}U) ratios vary positively with (^{231}Pa)/(^{235}U) ratios, but negatively with (^{226}Ra)/(^{230}Th) ratios (*18, 26*). These relations are consistent with the notion that the systematics of Th, U, and Pa, but not ^{226}Ra, depend on the degree of melting.

Assuming homogeneous sources, we can explain in two ways the observation that Th isotope ratios are lower and associated with greater Th-U disequilibria in the Endeavor than in the Juan de Fuca samples: (i) a long melting time [~250,000 years to reach 15% melting in the southern Juan de Fuca segment using the parameters of (8)], instantaneous ascent, and an initial Th activity ratio in the source [$(Th)_s$] ~1.3; or (ii) instantaneous melting, ascent for ~39,000 years, and $(Th)_s$ ~1.5 (*4*). Although any of the three parameters in each set may vary, the first combination is preferable because it better fits the observed global relation of Th and Sr isotopes (Fig. 3) and the second is inconsistent with the presence of excess ^{226}Ra. The inverse relation between excess ^{230}Th and excess ^{226}Ra

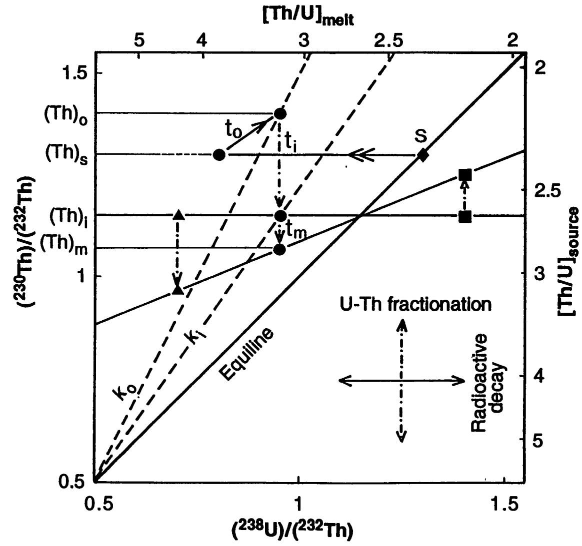

Fig. 1. Schematic (^{230}Th)-(^{238}U) isochron diagram. Although it refers specifically to the ^{238}U-^{230}Th pair, it can be generalized to all parent-daughter pairs in the three decay schemes. Disequilibrium occurs by fractionation of ^{230}Th from ^{238}U during partial melting. Magma is produced by the process of melting source S (diamond), which is isotopically homogeneous at the scale of melting and initially in radioactive equilibrium (that is, on the equiline) with $(Th)_S$. If $D_{Th} < D_U$, then (^{238}U)/(^{230}Th), or k, is <1.0 in the melt (solid circles). As the degree of melting increases, the ^{230}Th enrichment and [Th/U] ratio in the melt decrease. Here the degree of melting is insufficient for the $[Th/U]_{melt}$ to decrease to the $[Th/U]_{source}$. At the end of melting (after time t_0), the (^{230}Th)/(^{232}Th) ratio in the melt is $(Th)_0$, which exceeds $(Th)_S$ if t_0 is long. The $[Th/U]_{melt}$ remains constant after the melt ceases to be in chemical equilibrium with its source, but the (^{230}Th)/(^{232}Th) ratio decreases during transfer time t_i to $(Th)_i$ at the time of eruption as the result of unsupported radioactive decay. The ^{230}Th enrichment decreases from k_0 at the end of melting to k_i at the time of eruption. Near the time of eruption the melt precipitates phenocrysts, for some of which $D_U < D_{Th}$ (solid triangles) and for others of which $D_{Th} < D_U$ (solid squares). There is isotopic homogeneity, with all phases having $(Th)_i$. During the time between eruption and measurement (t_m), all phases evolve toward radioactive equilibrium by pivoting around $(Th)_i$ on the equiline so that the bulk sample has $(Th)_m$ when measured. In this case, t_m is the conventional age of the lava.

suggests that smaller melt fractions require longer ascent times.

These conclusions can be challenged for several reasons. First, the ^{230}Th enrichments are compatible with currently accepted values for ϕ during mantle melting of 0.5 to 2% if D_{Th} ~0.005 and D_U ~0.0015 (8). However, models that assume chemical equilibrium between silicate solids and liquid cannot account for the magnitude of the ^{230}Th enrichments if D's are more similar than these. They are even less able to explain the greater magnitude of the ^{226}Ra and ^{231}Pa enrichments. For example, if $(^{226}\text{Ra})/(^{230}\text{Th}) = 3.0$, then $\phi = D_{Th}/2$ (39); the required ϕ is absurdly low if $D_{Th} \sim 0.005$. Second, ^{230}Th enrichments do not correlate globally with other measurements of melt fractions (3) or even within the Endeavor segment itself (18), although they are generally greater in oceanic alkali basalts than in MORBs (Fig. 4). Finally, excess ^{230}Th is inconsistent with experimental measurements of D's for clinopyroxene, which has the highest Th and U contents of major mantle minerals (40).

The problems that affect interpretation of radioactive disequilibria also apply to other aspects of igneous chemistry and can be generalized as follows: (i) distinguishing effects of partial melting from alteration and differentiation; (ii) acquiring better values of D's for highly incompatible elements; (iii) distinguishing effects of variable degrees of melting from earlier source enrichments and depletions; and (iv) evaluating the effects of refractory accessory phases, chemically open sources, and chemical disequilibrium during melting. We discuss each below.

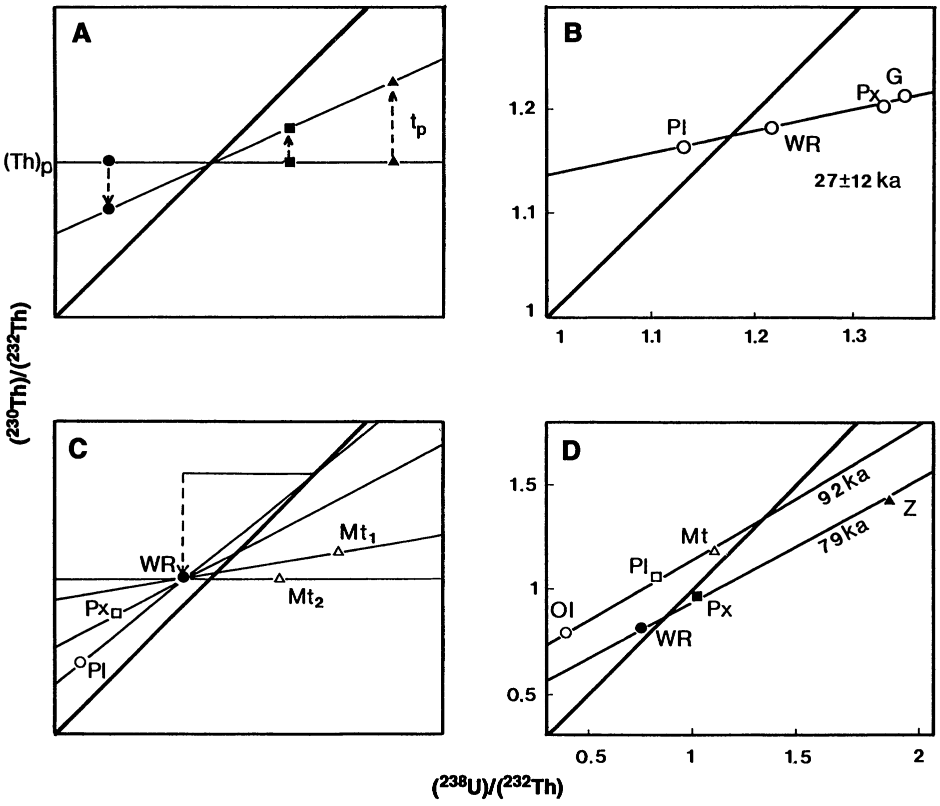

Fig. 2. U-Th isochron diagrams illustrating differentiation processes. (**A**) Schematic results for three phases that had the same initial isotope ratio, $(\text{Th})_p$, formed at the same time (t_p), and remained closed systems since. If they formed near the time of eruption, then $(\text{Th})_i = (\text{Th})_p$, $t_p \sim t_m$, the same case as the inclined line through $(\text{Th})_i$ in Fig. 1. (**B**) Mass spectrometric data for the youngest basalt from Mount St. Helens volcano, for which t_m = 2000 years but t_p = 27,000 years (25). Pl, plagioclase; WR, whole rock; Px, pyroxene; G, ground mass; ka = 1000 years. Interpretation is not simple because these same phases have excess ^{226}Ra, there are mass-balance inconsistencies with the data, and crustally derived dacites from the same volcano do not show apparent $t_p > t_m$ relations. (**C**) Schematic results for a hypothetical historical volcanic rock (WR) in which the crystallization sequence was plagioclase, pyroxene, and magnetite (Mt), and the time interval between the saturation of each phase (t_i) was long. $(\text{Th})_0$ is shown by the solid line, and t_i by the dashed line. Only magnetite (Mt_2) precipitated again at the time of eruption. (**D**) Alpha spectrometric data for phenocrysts from an andesite of Santorini volcano (61). Ol, olivine, and Z, zircon. The high [Th/U] ratio in olivine is attributed to apatite inclusions. The thin upper line connects the phenocrysts attributed to a basaltic mixing component; the thin lower line does the same for a dacitic component, including its Fe-rich pyroxenes. Again, interpretation is not simple because the $(\text{Th})_i$ values for the two magmas differ to a suspicious extent, and apatite saturation is required in the basalt.

Alteration is not a general problem because researchers using different samples and selection criteria obtain similar results (2, 3) and methods for cleaning submarine samples appear to be successful (30). Differentiation processes usually have only minor effects on bulk rock disequilibria in basalts and andesites, but assimilation of hydrothermally altered wall rocks might fractionate ^{238}U, ^{230}Th, and ^{226}Ra without affecting other isotopes significantly (40, 41).

Differences in very small D's are difficult to measure. Values of D_U, D_{Th}, and D_{Ba} are less than 0.02 for olivine-pyroxene residua (3, 40), but differences between them and their functional dependence on temperature, pressure, oxygen fugacity, and composition remain speculative. For clinopyroxene, for example, D_U is less than D_{Th} under the oxidizing conditions applicable to subduction zones and perhaps even under the conditions of magma genesis at ocean ridges and islands, but the uncertainties for the latter are almost as large as the differences (40). If chemical equilibrium exists, D_{Th} must be usually less than D_U because enrichment of ^{230}Th is too ubiquitous to be explained by contamination and the mantle has become depleted in Th with time (42). However, higher D_U may be a result of refractory accessory phases.

Old source enrichments and small degrees of melting both produce melts rich in incompatible elements. The two processes usually cannot be distinguished, especially if old enrichments are introduced by small degree melts. However, their effects are not cumulative for radioactive disequilibria, which may explain the lack of global correlation between element concentrations and disequilibria.

The melting behavior of accessory minerals may be important in generating disequilibria (4, 30). An accessory phase that is consumed during batch melting has essentially no effect on magma chemistry because its elements are repartitioned between refractory phases and larger degree melts. However, if melts from relatively undepleted sources containing refractory accessory minerals routinely blend with melts from sources lacking them, then trace element ratios may be determined by the accessory phases even though major elements will be determined by the average melt fraction of the entire column (43). Accessory minerals that may coexist with small degree melts in the mantle include several that typically have quite high [Th/U] ratios (for example, phlogopite, amphibole, sphene, and whitlockite) and others that have quite low [Th/U] ratios (zircon and possibly garnet) (3).

Open sources may be necessary to explain large disequilibria created during partial melting (2, 33, 44). In an open system, fluids preferentially transport the enriched nuclide to the source and cause melting at the vapor present solidus, or subsolidus vapor is extracted from the surroundings of a partially molten region. In either case, a fluid phase beside silicate melt is involved in magma genesis.

The preceding discussion made a sharp distinction between melting accompanied by chemical equilibrium between melt and matrix versus ascent without it (Fig. 1). However, the two need not be so distinct. Melt can acquire large radioactive disequilibria in two ways if the melt and matrix react without achieving chemical equilibrium. First, melts can inherit the disequilibria of an accessory phase if the source is isotopically homogeneous and the accessory phase has an extremely large or small parent/daughter ratio and dominates the low-melting fraction (*4, 19*). Second, the melt will become enriched in the faster diffusing nuclide if diffusion coefficients differ significantly. The lability of short-lived nuclides in radiation-damaged sites and recoil effects from surface to melts may enhance nonequilibrium phenomena.

Although reasons for disequilibria in each case or for differences between tectonic environments cannot yet be specified, some tentative conclusions are suggested. The increase in k from lamproites to alkali basalts to tholeiites reflects increasing degrees of melting. The apparent increases in k from mid-ocean ridge to ocean island to island arc tholeiites and from oceanic to continental alkali basalts parallel an expected increase in mantle f_{O_2} (*45*) and may be a result of decreasing D_U (*3*). If related to melting, the greater Ra enrichments at active plate margins indicate that the open systems or permeable flow conditions characteristic of divergent and convergent margins are absent within plates. This result, in turn, suggests either that subsolidus fluid is absent at sites of intraplate melting or that melts at active plate boundaries can be extracted at smaller porosities than in other areas. This second possibility might exist if shear rather than buoyancy forces are primarily responsible for melt migration at active margins (*1*).

Thorium isotopes and Ra-Th disequilibria also show that ascent time is less than 10,000 years for many oceanic basalts. Some excess ^{226}Ra [half-life ($t_{1/2}$) = 1600 years] is present in most basalts regardless of tectonic environment, whereas excess ^{228}Ra ($t_{1/2}$ = 5.8 years) is absent (*2, 3*). Consequently, most basalts erupt within 30 to 8000 years after partial melting ceases. A similar upper bound on t_i (ascent time) comes from the constancy of $(\mathrm{Th})_i$ of lavas at individual volcanoes or in local regions when accompanied by disequilibria between ^{238}U and ^{230}Th (*2, 46*). If the source has homogeneous [Th/U] but melts have $k \neq 1.0$, then $(\mathrm{Th})_i$ in melts will depart from $(\mathrm{Th})_0$ whenever t_i is long enough to modify (^{230}Th). How long this takes depends on the magnitude of $(\mathrm{Th})_0$ and k. If $(\mathrm{Th})_0 = 1.0$ and $k = 0.9$, for example, then constancy of $(\mathrm{Th})_i$ to ± 0.01 requires that the melts ascend to the surface within <10,000 years. Use of mass spectrometry can reduce this constraint on ascent times to a few millennia. Similarly, if $D_{Ra} = D_{Ba}$ and the [Ba/Th] ratio of the source is constant, then the (^{226}Ra)/(^{230}Th) ratios of magmas at the end of partial melting can be estimated from their [Ba/Th] ratios. The t_i estimated in this way for some MORBs is about 1000 years if the [Ba/Th] source ratio is 8 (*47*).

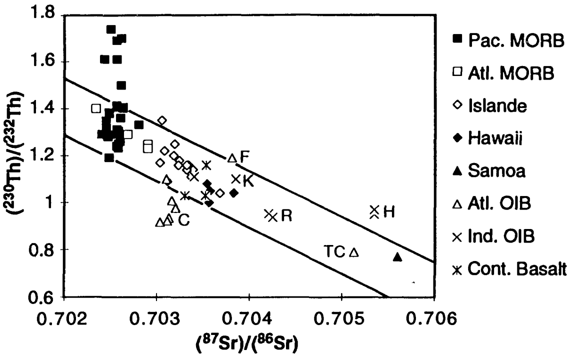

Fig. 3. Sr and Th isotope correlation for MORB from neovolcanic zones and intraplate basalts less than 10,000 years old. Icelandic basalts with δ^{18}O < 5.0 per mil have been excluded because their Th isotope ratios have been modified by assimilation (*68*). Hyperalkalic mafic rocks from Africa also have been excluded for simplicity. Atlantic (Atl.) and Indian (Ind.) OIBs are identified as follows: C, Tenerife and Lanzarote (Canary); F, Faial (Azores); H. Heard; K, Karthala (Comores); R, Reunion; TC, Tristan da Cunha; Pac., Pacific; and Cont., continental. Data are from sources listed in (*3, 18, 28, 36, 37, 47, 49, 67, 72*). The Th-Sr correlation band is the best fit to the data, except for MORB with $(\mathrm{Th})_i$ > 1.41 and the results for Canaries and Heard.

The magmas that erupt the soonest after their last major chemical fractionation are, not surprisingly, the least viscous: the Na-carbonatites of Oldoinyo Lengai volcano, Tanzania, which has erupted twice in the last 35 years. Both times the magma contained excess ^{228} and ^{226}Ra. Estimates of magma age ($t_1 + t_0$) depend on how Ra and Th fractionated during its formation. If the carbonatite magma formed by rapid exsolution from a silicate magma, then the age of the parental magma is unknown but the exsolution began a mere 7 to 20 years before eruption, shortly after the last eruption. If fractionation is more gradual, the magma age can double (*14*). Although excess Ra can be sustained by radioactive decay in a steady state carbonatite magma chamber (*48*), the inverse relation between the (^{228}Ra)/(^{226}Ra) ratio and repose time observed at Lengai is better explained by formation of new carbonatite before each eruption.

The size and ubiquity of radioactive disequilibria in basaltic rocks have contributed to a substantial reconception of partial melting processes and have facilitated quantification of melting times and magma ascent. Extraction of small melt fractions seems to be possible and common, and magma sources at active plate boundaries may differ from those within plates with respect to the presence or absence of a free vapor phase or the characteristics of the melt flow regime. The t_0's for basaltic magmas might be several hundred millennia, whereas t_i's are a few decades to millennia. The difference between the two regimes is the respective times when the last major chemical fractionation between the nuclides occurred.

Differentiation Processes and Time Scales

Fractional crystallization results in relatively little separation of Th, U, and Ra in most magmas. Significant fractionation of Th from U does not occur until accessory phases such as magnetite, zircon, apatite, or sphene precipitate. Variation in the [Th/U] ratio is slight even then because the mass fraction of accessory minerals is small. Ratios of [Th/U] increase by less than 20% in rhyolites because zircon is removed (*49, 50*) and decrease by about the same amount in trachytes because of sphene fractionation (*51*). Plagioclase and especially alkali feldspar concentrate Ra relative to Th, and their removal depletes the melt in Ra (*24, 25, 52*). Feldspars also are enriched in ^{210}Pb relative to ^{226}Ra; this ^{210}Pb enrichment in whole rocks may reflect feldspar accumulation (*17*).

Vapor exsolution affects the physics of magmatic differentiation and the geochemistry of volatile elements. Preferential removal of U from magma by hydrous fluids has been invoked to explain both a large range in [Th/U] ratios (up to 11) in subcontemporaneous ultrapotassic rocks (*53*) and [Th/U] ratios higher in syenite nodules than in their otherwise chemically identical trachyte hosts (*54*). However, vapor fractionation in magmas primarily affects the end products of the ^{238}U decay chain, ^{210}Po and ^{210}Bi, and can be used in the study of the residence time of degassed melt branches in shallow reservoirs (*55*).

Assimilation of wall rocks by magmas

seems to have variable but minor effects on disequilibria in the U series, at least in subaerially erupted magmas. Thorium isotope ratios may decrease by as much as 20% from alkali basalts to contemporaneous hawaiites as a result of assimilation in the Chaine des Puys (French Massif Central), but the extent of variation in uncontaminated parents is unknown (*56*). Sufficient assimilation to raise the $^{18}O/^{16}O$ ratio by about 0.5 per mil and $^{87}Sr/^{86}Sr$ ratios by >0.001 had no effect on disequilibria between ^{226}Ra, ^{230}Th, and ^{238}U or on Th isotope ratios in two andesites (*57, 58*). However, assimilation of oceanic crust that was hydrothermally altered might be responsible for high (^{230}Th)/(^{232}Th) or (^{226}Ra)/(^{230}Th) ratios in MORB (*41*).

In contrast to the limited information provided about differentiation, analysis of short-lived radionuclides is likely to become a powerful tool in the evaluation of magma mixing, a potential that is evident even in studies of bulk samples. For example, it is difficult to distinguish between the role of crystal fractionation and that of crustal melting in the genesis of silicic magmas in Iceland because the two processes have the same isotopic consequences for most elements. However, Th isotope ratios are higher in Icelandic basalts and andesites than in dacites and rhyolites. Because differentiation times are too short to account for the difference, incorporation of a crustally derived silicic magma is required. Thorium is the only radiogenic isotope that changed quickly enough in the crust to differ (*49*). The lower $(Th)_i$ reflects the higher [Th/U] of the crustal rather than of the mantle sources. Similarly, the variations in (^{226}Ra)/(^{230}Th) ratios between 1950 and 1983 in lavas from Etna are best understood by the mixing of two magmas: one differentiated with a low (^{226}Ra)/(^{230}Th) ratio (~1.7) and a more recent, more mafic one with a higher (^{226}Ra)/(^{230}Th) ratio (>2) (*15*).

However, minerals have the best magmatic memory in volcanic rocks, and results of disequilibria studies highlight the difficulty distinguishing phenocrysts, which precipitated from their host melts, from xenocrysts, which are foreign to and older than the host melt. Studies of common minerals are difficult, however, because their Th and U contents are low. Several grams of mineral separates are typically necessary for alpha spectrometry. As sample size is reduced with mass spectrometry, mineral studies will increase in number and quality. When they are combined with studies of chemical diffusion and crystal growth, the complex history of magmas will further unfold.

Mineral data are usually analyzed with isochron diagrams such as (^{230}Th)/(^{232}Th) versus (^{238}U)/(^{232}Th) (Fig. 2). In this context, another important event during the history of volcanic rocks needs to be specified, namely, when their phenocrysts form. The Th activity ratio of the melt at the time of phenocryst precipitation is $(Th)_p$, and t_p is the time interval between phenocryst precipitation and measurement (the age of the phenocrysts). If the phenocrysts evolve as a closed system after precipitation, then their plot will form an isochron whose slope is $1 - e^{-\lambda t}$, where t is t_p. If the interval between phenocryst crystallization and eruption ($t_p - t_m$) is short compared to the half-life of ^{230}Th [less than a few millennia, as expected from crystal growth rates of around 10^{-10} cm/s (*59*)], then the time indicated by the isochron is the conventional age of the rock, or time since eruption. Determining t_m was the original motivation for development of this research field, and the prerequisite initial Th isotopic homogeneity has been found in zero-age rocks with the precision of mass spectrometry and alpha spectrometry (*24, 25, 33, 60*).

In the simplest case (Figs. 1 and 2A), all crystals are phenocrysts that crystallized at the same time with the same (^{230}Th)/(^{232}Th) ratio (isotopic homogeneity). However, neither initial isotopic homogeneity nor subsequent closed system behavior is ubiquitous and neither can be safely assumed, especially in petrologically complex samples. Isotopic heterogeneity among crystals or between crystals and groundmass indicates either that $t_p - t_m$ is appreciable or that the system has been open. The very heterogeneity that complicates measurement of the eruption age can be used to evaluate the pre-eruption history of the magma. Two examples from Mount St. Helens (*25*) and Santorini (*61*) are illustrated and discussed below (Fig. 2, B to D).

The age from the slope may significantly exceed the independently determined eruption age (that is, $t_p > t_m$) and, therefore, include appreciable time before eruption (Fig. 2B). This age (t_p), the time since the last diffusive equilibrium between phenocrysts and melt, may underestimate the time since phenocryst nucleation and is analogous to a closure age in the geochronology of metamorphic rocks. Phenocrysts in basalts to rhyolites sometimes yield apparent internal isochrons that give ($t_p - t_m$) values of 10^3 to 10^5 years (*25, 50, 62*).

Magmatic differentiation may last long

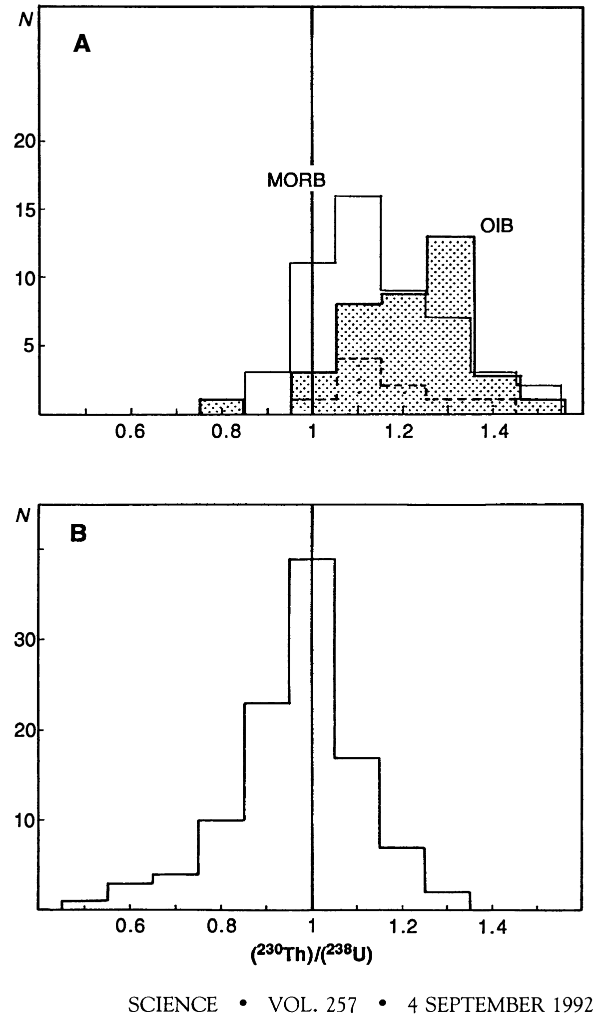

Fig. 4. (^{230}Th/^{238}U) ratios in (**A**) oceanic basalts (MORB and OIB) and (**B**) subduction zone basalts and andesites. When the same ratio was measured for historical products of the same volcano, only one is plotted. In (A), the dashed line in the stippled field of OIBs refers to the tholeiites of Hawaii and Iceland and the solid line refers to transitional and alkali basalts. Data are from the same sources as in Figs. 3 and 4.

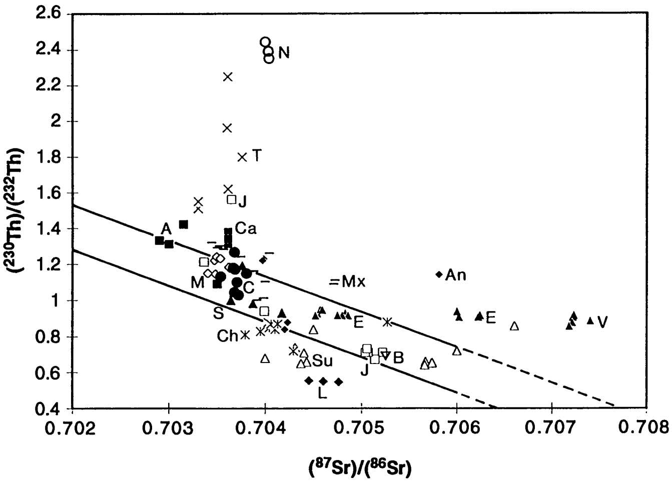

Fig. 5. Sr and Th isotope correlation for basalts and andesites less than 10,000 years old from subduction zones. Different arc segments are shown by different symbols that are identified by letters as follows: A, Aleutians; An, Antilles; B, Banda; C, Costa Rica; Ca, Cascades; Ch, Chile; E, Eolian; J, Japan (including Bonins); L, Luzon; M, Marianas; Mx, Mexico; N, Nicaragua; S, Sangihe; Su, Sunda; T, Tonga; V, Vesuvius. Data are from sources listed in (*3, 20, 57, 72*). The Sr-Th correlation band is from Fig. 3.

enough that phenocrysts never equilibrate isotopically with respect to short-lived nuclides. Figure 2C illustrates a hypothetical example in which significant time elapsed between saturation, or closure, of different mineral phases. Deviations from the isochron that were defined by the first mineral to crystallize could date the subsequent crystallization sequence. No such integration of petrology and U-series disequilibria has yet been achieved, but crystal growth rates are fast enough that this effect is more likely to be evident in the systematics of (^{226}Ra) and (^{230}Th).

Much of the observed heterogeneity in Th isotope ratios among crystals has been attributed to mixing of minerals from diverse magmas (*25, 63*). A Santorini andesite is a possible example of binary mixing (Fig. 2D). Here, dacitic and basaltic mineral assemblages in the same rock seem to define separate isochrons of similar slope but different Th isotope ratios (*61*).

Isochrons between $(^{226}Ra)/[Ba]$ and $(^{230}Th)/[Ba]$ ratios are well suited to the short differentiation times that we inferred in the previous section. Feldspar-glass Ra-Th isochrons for samples from the phonolite lava lake at Erebus volcano, Antarctica, indicate that the cores of the large feldspar crystals were about 2400 ± 250 years old upon eruption (*24*). In addition, the presence of excess ^{228}Ra with respect to ^{232}Th in these crystals indicates that their rims grew within years of eruption while floating in the lava lake. Ratios of higher $(^{226}Ra)/[Ba]$ for bulk rocks than for minerals in recent andesites and dacites that erupted from Mount St. Helens volcano suggest that some phenocrysts formed 500 to 3000 years before eruption or that the magma reservoir was recharged by ^{226}Ra-enriched melts (*25*). These "old" phenocrysts still have the same Th isotope ratios as the bulk sample [homogeneous $(Th)_p$].

Time scales of differentiation can be studied with whole rocks as well as minerals. Differences in initial Th isotope ratios between parental magma and differentiates constrain time in a closed system, but suitably young eruptions of related parents and differentiates from the same volcano are uncommon. Chemically zoned eruptions provide examples of this relation. Pumices from the Fogo A eruption of Sao Miguel, Azores, exhibit homogeneous initial Th isotope ratios despite an estimate of 75% crystallization of mafic trachyte that yields 2 km^3 of differentiate; therefore, 6 km^3 of magma crystallized in <10,000 years, primarily on sidewalls (*52, 54*). However, data for whole rocks sometimes define isochrons of a few millennia to 60,000 years in phonolitic and rhyolitic systems (*50, 51*). These plots record minimum differentiation times unless unrelated materials have mixed.

Differentiation times also can be calculated if one infers the $(^{230}Th)/(^{232}Th)$ of the parent magma from the initial Th isotope ratio of young nearby basalts, or from the plot in Fig. 3 if the Sr isotope ratio of older basalts is known. This approach suggests that differentiation from alkali basalt to trachyte or phonolite at large intraplate volcanoes with calderas typically takes 10^4 to 10^5 years (*24, 52*). The decrease of excess ^{226}Ra from basalt through andesite to dacite in arcs, and in increasingly differentiated lavas at Etna and Batur volcanoes, indicates that the differentiation time in these systems is at most a few thousand years (*15, 17, 32–34*).

Radium, thorium, and uranium are separated more during partial melting than in crystal fractionation or assimilation of continental crust. Consequently, radionuclides constrain the time scale of differentiation better than these processes but are likely to become powerful tools for studying magma mixing. Ratios of $(^{230}Th)/(^{232}Th)$ and $(^{226}Ra)/(^{230}Th)$ can provide time resolution on scales of centuries to millennia. Differentiation time scales increase with melt viscosity. Carbonatites erupt within years of formation. Andesites and trachytes often form within a few millennia, but phonolites and rhyolites erupt tens of thousands of years after their last major chemical fractionation.

Thorium Isotopes and Magma Sources

The isotopes of Sr and Pb in magmatic rocks have been used for 30 years to characterize magma sources. They respond to the magnitude and duration of variations in the ratios of Rb/Sr and either U/Pb and Th/Pb, respectively, in magma sources. For example, high $^{87}Sr/^{86}Sr$ ratios in basalt indicate that the source of Sr had high time-integrated Rb/Sr ratios and is likely to include the crust or subcontinental mantle, whereas high $^{207}Pb/^{204}Pb$ ratios indicate that the source of Pb had a high U/Pb ratio during the first half of the earth's history when ^{235}U was most abundant. These valuable isotopic tracers were joined by Nd more than a decade ago as a result of instrumental improvements in mass spectrometry that facilitated recognition of multiple mantle source components (*64*). Further improvements have allowed Th, Hf, and Os to become additional isotopic tracers, with Th as the most incompatible of them all.

Isotopes of Th and Sr in oceanic basalts have an inverse relation (*11*) (Fig. 3). The same is true for Nd and Sr isotopes (*64*). The similarity between Th-Sr and Nd-Sr correlation diagrams indicates that Th/U, Rb/Sr, and Nd/Sm ratios covary in the source components. Consequently, Th, Rb, and Nd have been depleted with respect to U, Sr, and Sm, respectively, in the mantle. Continental lithosphere (crust and mantle) forms the enriched complementary reservoir (*37, 65*).

There is greater scatter in Th-Sr than in Nd-Sr isotopic correlations for several reasons that affect Th more than Sr or Nd isotopes: (i) prolonged melting, (ii) slow ascent, (iii) nonlinear effects of mixing, and (iv) large or recent variations in the parent/daughter ratio of the source.

Slow-continuous or sequential-fractional melting (that is, with an appreciable t_0) can raise $(Th)_0$ without affecting $^{87}Sr/^{86}Sr$, which may explain the anomalously high Th isotope ratios for some MORBs, unless these values are due to alteration or assimilation (*8, 16, 30*).

Atypically long ascent times may help explain samples at the bottom or below the Th-Sr isotope correlation band, none of which are known to have large ^{226}Ra excesses. Whenever $k < 1.00$ but ascent times exceed 10,000 years, Th isotope ratios decrease in the magma. Basalts that erupted near a large caldera on Sao Miguel, Azores, had initial Th isotope ratios about 7% lower than predicted from local variations in Sr isotopic composition; their ascent may have been slowed by density anomalies beneath the caldera (*66*).

Isotope correlations among Sr, Nd, Pb, and Hf are generally interpreted as the result of multicomponent mixing of mantle sources. Even if the isotopic compositions of the source components are in the mixing array, mixtures of the components need not be if the concentration ratios of the tracer elements differ greatly among components. This process may explain $(\mathrm{Th})_i$ below the Sr-Th correlation band in ocean islands such as Tenerife and Lanzarote in the Canary Islands (*67*). Also, Th and He are the isotopic tracers most likely to be determined by an introduced fluid rather than by the matrix through which the fluid passes, because these tracers are the most incompatible.

Magma mixing and assimilation of crustally derived components also contribute to scatter, even in oceanic islands. Although other radiogenic isotopes are usually unaffected unless seawater, sediment, or old continental crust is present, Th isotopes rapidly reflect differences in trace element ratios between the mantle and the rocks that are derived from it. For example, some quartz tholeiites from Iceland plot below the Th-Sr isotope correlation band because they have been contaminated by old hydrothermally altered mafic rocks with relatively lower $(^{230}\mathrm{Th})/(^{232}\mathrm{Th})$ ratios (*68*).

Mantle sources may differ more in Th than in other isotopes because either Th responds faster to changes in parent/daughter ratios or because Th-U fractionation is greater than for other parent/daughter ratios in the decay scheme. The second possibility is especially likely if the source has extensively interacted with fluids composed of C, H, O, and halogens. Atypically high Th isotope ratios at low $^{87}\mathrm{Sr}/^{86}\mathrm{Sr}$ ratios may be the result of carbonate alteration in the mantle [for example, at Nyiragongo volcano (*37*)] because U partitions strongly into fluids in $\mathrm{CO_3}^{2-}$ (*14, 37, 69*). Conversely, atypically low Th isotope ratios at high $^{87}\mathrm{Sr}/^{86}\mathrm{Sr}$ ratios indicate the presence of phlogopite in the mantle [for example, at Gaussberg volcano (*19*)]. These obvious examples of mantle alteration do not appear in Fig. 3, but the process may contribute to the location of data for Faial and Heard, for example.

This sensitivity of fractionation between U, Th, and Ra to the nature and behavior of fluids also makes Th isotopes and disequilibria useful in studies of magma genesis at subduction zones. Almost half of subduction zone volcanic rocks lie within the Th-Sr isotope correlation band (Fig. 5), and a similar proportion lies within the Th-Pb isotope array (*2, 3, 20, 33*). Consequently, no exotic sources of Th, Sr, or Pb (for example, pelagic sediment) are required in these rocks even though these fluid-mobile elements are often enriched relative to the rare earth elements. This proscription of sediment exists because the [Th/Sr] ratio is at least 30 times higher in clay than in the depleted mantle, and Th/U ratios are higher in clays than in the mantle for the same Pb isotopic composition. The addition of even 1 or 2% sediment would move mixtures out of the Sr-Th correlation band. Such mixtures may, however, account for $(\mathrm{Th})_i$ below the Sr-Th array in the Sunda (Indonesia), southwest Japan, Luzon (Philippines), and South Chile arcs (*2, 17, 20, 33, 57, 58*). In South Chile, $(^{238}\mathrm{U})/(^{230}\mathrm{Th})$ ratios correlate positively with $^{10}\mathrm{Be}/^{9}\mathrm{Be}$, indicating that the added sediments were subducted recently (*70*).

Samples from several oceanic arcs plot above the Sr-Th array. Ratios of $(^{230}\mathrm{Th})/(^{232}\mathrm{Th})$ rather than of $(^{238}\mathrm{U})/(^{230}\mathrm{Th})$ correlate positively in these cases with $^{10}\mathrm{Be}/^{9}\mathrm{Be}$ such as in lavas from the Bismarck arc (*34*), indicating that the high $(\mathrm{Th})_i$ values are related to recent subduction of young sediment. The difference in Th isotopes between the Bismarck and South Chile arcs is attributed to variations in the residence time of slab-derived, fluid-mobile elements in the mantle wedge. Rapid transfer of Th (as well as Be and U) from the slab to the surface characterizes the slowly convecting subcontinental mantle wedge beneath South Chile. In contrast, transfer beneath the Bismarck arc is slowed by its more rapid downward convection of the mantle wedge matrix associated with formation of the adjacent back-arc basin, so that the Th in Bismarck arc magmas comes from the metasomatized mantle wedge rather than from the slab itself (*34*).

Lavas in both the South Chile and Bismarck arcs are enriched in U. However, almost 40% of arc magmas show no significant U-Th fractionation ($k = 1.00 \pm 0.05$), in contrast to MORBs and oceanic island basalts (OIBs) (Fig. 4). The apparent absence of U-Th fractionation in many arc lavas may reflect intermediate conditions between those of mid-ocean ridges and those of subduction zones that show U enrichment [for example, intermediate f_{O_2} (*33*)]. Alternatively, the Th and U budget of many arc sources may be determined by minerals that precipitated from slab-derived fluids. If these secondary minerals are old enough to be in secular equilibrium before melting, then their [Th/U] and $(^{230}\mathrm{Th})/(^{232}\mathrm{Th})$ ratios will equal those of the melt if $D_{\mathrm{U}} \sim D_{\mathrm{Th}}$ or melting is fast enough to avoid chemical equilibrium with the residue. Either condition would cause the lack of U-Th fractionation over a wide range of Th isotope ratios in arcs (*71*).

Although Th isotope systematics appear similar to those of moderately incompatible isotopic tracers (Nd and Hf), there is greater scatter in Th isotopes than can be accounted for by the effects of ascent and differentiation. Prolonged melting may explain high Th isotope ratios in depleted MORBs and arc basalts, but at least some of the latter are demonstrably related to subduction. Mixing between magma sources may explain atypically low Th isotope ratios in both OIB and arcs. Carbonate metasomatism may occur in both environments, can fractionate U from Th more than other parent-daughter pairs, and may be responsible for some high Th isotope ratios. Combined studies of U series and $^{10}\mathrm{Be}$ show that slab dehydration leads to eruptions in less than 20,000 years in some subduction zones, whereas in others it results in subsolidus metasomatism that only later contributes to magma genesis.

REFERENCES AND NOTES

1. M. Spiegelman and D. McKenzie, *Earth Planet. Sci. Lett.* **83**, 137 (1987); N. Ribe, *J. Volcanol. Geotherm. Res.* **33**, 241 (1987).
2. M. Condomines, C. H. Hemond, C. J. Allègre, *Earth Planet. Sci. Lett.* **90**, 243 (1988).
3. J. Gill, D. Pyle, R. Williams, in *Uranium Series Disequilibrium: Applications to Environmental Problems*, M. Ivanovich and R. S. Harmon, Eds. (Clarendon, Oxford, ed. 2, 1992), chap. 7.
4. J. Gill, *Proc. R. Soc. London Ser. A*, in press.
5. M. Ivanovich and R. S. Harmon, Eds., *Uranium Series Disequilibrium: Applications to Environmental Problems* (Clarendon, Oxford, ed. 2, 1992).
6. See (*3*) and (*40*) for recent compilations of partition coefficients. Diffusion coefficients for Th, U, Pa, and Ra in silicates are poorly known but are likely to be 10^{-14} to 10^{-20} m^2/s in the mantle [R. Freer, *Contrib. Mineral. Petrol.* **76**, 440 (1981)], to be slower for highly charged cations than for alkaline earths [J. H. Bédard, *Earth Planet. Sci. Lett.* **91**, 359 (1989)], and to vary with f_{O_2} [A. J. Jurewicz and E. B. Watson, *Contrib. Mineral. Petrol.* **99**, 186 (1988)].
7. M. Spiegelman and P. Kenyon, *Earth Planet. Sci. Lett.* **109**, 611 (1992); T. Iwamori, *Geophys. Res. Lett.* **19**, 309 (1992).
8. R. Williams and J. Gill, *Geochim. Cosmochim. Acta* **53**, 1607 (1989).
9. J. Joly, *Philos. Mag.* **18**, 577 (1909); K. Kigoshi, *Science* **156**, 932 (1967); C. J. Allègre, *Earth Planet. Sci. Lett.* **5**, 209 (1968).
10. C. J. Allègre and M. Condomines, *Earth Planet. Sci. Lett.* **28**, 395 (1976); *Nature* **299**, 21 (1982).
11. M. Condomines, P. Morand, C. J. Allègre, *Earth Planet. Sci. Lett.* **55**, 247 (1981).
12. M. Condomines, J. C. Tanguy, G. Kieffer, C. J. Allègre, *Geochim. Cosmochim. Acta* **46**, 1397 (1982).
13. G. Capaldi, M. Cortini, P. Gasparini, R. Pece, *J. Geophys. Res.* **81**, 350 (1976).
14. R. Williams, J. Gill, K. Bruland, *Geochim. Cosmochim. Acta* **50**, 1249 (1986).
15. M. Condomines *et al.*, *Nature* **325**, 607 (1987).
16. K. Rubin and J. Macdougall, *ibid.* **335**, 158 (1988).
17. K. Rubin *et al.*, *J. Volcanol. Geotherm. Res.* **38**, 215 (1989); M. Reagan, *Eos* **69**, 1509 (1988).
18. S. J. Goldstein, M. T. Murrell, D. R. Janecky, *Earth Planet. Sci. Lett.* **96**, 134 (1990); S. J. Goldstein,

M. T. Murrell, D. R. Janecky, J. R. Delaney, D. A. Clague, *ibid.* **109**, 255 (1992); A. M. Volpe and S. J. Goldstein, in preparation.

19. R. Williams, K. Collerson, J. Gill, C. Deniel, *Earth Planet. Sci. Lett.*, in press.
20. F. McDermott and C. Hawkesworth, *ibid.* **104**, 1 (1991).
21. A. Zindler *et al.*, abstract for paper presented at the 7th International Congress of Geochemistry, Canberra, Australia, 1990.
22. A. S. Cohen and R. K. O'Nions, *Anal. Chem.* **63**, 2705 (1991); A. S. Cohen, N. S. Belshaw, R. K. O'Nions, *Int. J. Mass Spectrom. Ion Process.*, in press; Z. A. Palacz, P. A. Freedman, A. J. Walder, *Chem. Geol.* **101**, 157 (1992).
23. A. M. Volpe, J. A. Olivares, M. T. Murrell, *Anal. Chem.* **63**, 913 (1991).
24. M. Reagan, A. M. Volpe, K. V. Cashman, *Geochim. Cosmochim. Acta* **56**, 1401 (1992).
25. A. M. Volpe and P. E. Hammond, *Earth Planet. Sci. Lett.* **107**, 475 (1991).
26. R. Williams and R. E. Perrin, *Eos* **70**, 1398 (1989); R. Williams, M. T. Murrell, S. J. Goldstein *ibid.* **72**, 295 (1991).
27. P. W. Gast, *Geochim. Cosmochim. Acta* **32**, 1057 (1968); D. H. Green and A. E. Ringwood, *Contrib. Mineral. Petrol.* **15**, 103 (1967); J. F. Minster and C. J. Allègre, *ibid.* **69**, 37 (1978); A. W. Hofmann and M. D. Feigenson, *ibid.* **84**, 382 (1983).
28. S. Newman, R. C. Finkel, J. D. Macdougall, *Earth Planet. Sci. Lett.* **65**, 17 (1983); D. Ben Othman and C. J. Allègre, *ibid.* **98**, 129 (1990).
29. S. Krishnaswami, K. K. Turekian, J. T. Bennett, *Geochim. Cosmochim. Acta* **48**, 505 (1984).
30. I. Reinitz and K. K. Turekian, *Earth Planet. Sci. Lett.* **94**, 199 (1989).
31. D. McKenzie, *ibid.* **72**, 149 (1985).
32. G. Capaldi, M. Cortini, R. Pece, *Isot. Geosci.* **1**, 39 (1983).
33. J. Gill and R. Williams, *Geochim. Cosmochim. Acta* **54**, 1427 (1990).
34. J. Gill, J. Morris, R. Johnson, in preparation.
35. The primitive arc samples with excess ^{226}Ra are the 1982 basalt of Galunggung volcano, Java (*33*), and the 1965 basalt of Manam volcano, Papua New Guinea (*34*). The only primitive alkali basalt that has been studied is the 1790 Haleakala alkali basalt from Maui, Hawaii, which has 20% excess ^{266}Ra (*36*).
36. I. Reinitz and K. K. Turekian, *Geochim. Cosmochim. Acta* **55**, 3735 (1991).
37. R. Williams and J. Gill, *Geophys. Res. Lett.* **19**, 139 (1992).
38. J. K. Osmond and J. B. Cowart, in (*5*), chap. 9.
39. Equation 13 in D. McKenzie, *J. Geol. Soc. London* **144**, 299 (1987).
40. T. Z. LaTourrette and D. S. Burnett, *Earth Planet. Sci. Lett.* **110**, 227 (1992).
41. O. Sigmarsson, A. S. Cohen, R. K. O'Nions, *Eos* **72**, 574 (1991).
42. Evidence of progressive Th depletion in the mantle is from Pb isotopes in igneous rocks [C. J. Allègre, B. Dupré, E. Levin, *Chem. Geol.* **56**, 219 (1986)] and from Th/Sc ratios of sediments [S. R. Taylor and S. M. McLennan, *The Continental Crust: Its Composition and Evolution* (Blackwell, Oxford, 1985)],
43. E. Klein and C. H. Langmuir, *J. Geophys. Res.* **92**, 8089 (1987); B. Watson, J. M. Brennan, D. R. Baker, in *Continental Mantle*, M. A. Menzie, Ed. (Clarendon, Oxford, 1990), pp. 111–126; R. Varne, *Geology* **13**, 405 (1985); M. Reagan and J. Gill, *J. Geophys. Res.* **94**, 4619 (1989).
44. M. Cortini, in *Uranium Geochemistry, Mineralogy, Geology, Exploration and Resources*, B. DeVivo, F. Ippolito, G. Capaldi, P. R. Simpson, Eds. (Institution of Mining and Metallurgy, London, 1984), pp. 4–11.
45. S. E. Haggerty, in *Continental Mantle*, M. A. Menzies, Ed. (Clarendon, Oxford, 1990), pp. 87–109.
46. S. Newman, R. C. Finkel, J. D. Macdougall, *Geochim. Cosmochim. Acta* **48**, 315 (1984).
47. K. H. Rubin and J. D. Macdougall, *Earth Planet. Sci. Lett.* **101**, 313 (1990).
48. D. Pyle, J. B. Dawson, M. Ivanovich, *ibid.* **105**, 378 (1991).
49. O. Sigmarsson, Ch. Hemond, M. Condomines, S. Fourcade, N. Oskarsson, *Geology* **19**, 621 (1991); O. Sigmarsson, M. Condomines, S. Fourcade, *Contrib. Mineral. Petrol.*, in press.
50. D. Sampson, R. Williams, M. Robin, J. Gill, *Eos* **65**, 1128 (1984); D. Sampson, R. Williams, J. Gill, *ibid.* **66**, 388 (1985).
51. E. Widom and J. Gill, *ibid.* **72**, 574 (1991); B. Bourdon, A. Zindler, G. Worner, J. Rubenstone, *ibid.* **73**, 358 (1992).
52. E. Widom, H.-U. Schmincke, J. Gill, *Contrib. Mineral. Petrol.*, in press.
53. B. Villemant and C. Flehoc, *Earth Planet. Sci. Lett.* **91**, 312 (1989).
54. E. Widom, J. Gill, H.-U. Schmincke, *J. Petrol.*, in press.
55. G. Lambert, M. F. LeCloarec, B. Ardouin, J. C. LeRoulley, *Earth Planet. Sci. Lett.* **76**, 185 (1986); M. F. LeCloarec, G. Lambert, J. C. LeRoulley, B. Ardouin, *J. Volcanol. Geotherm. Res.* **28**, 85 (1986).
56. M. Condomines, P. Morand, G. Camus, J. L. Duthou, *Contrib. Mineral. Petrol.* **81**, 296 (1982).
57. O. Sigmarsson, M. Condomines, R. S. Harmon, J. D. Morris, *Nature* **346**, 163 (1990).
58. J. Gill, *Eos* **69**, 1509 (1988).
59. K. V. Cashman, in *Modern Methods of Igneous Petrology*, J. Nicholls and J. D. Russell, Eds. (Mineralogical Society of America, Washington, DC, 1990), pp. 259–314.
60. Ch. Hemond and M. Condomines, *J. Volcanol. Geotherm. Res.* **26**, 365 (1985).
61. D. Pyle, M. Ivanovich, R. S. J. Sparks, *Nature* **331**, 157 (1988).
62. T. Fukuoka, *Geochem. J.* **8**, 109 (1974).
63. A. Taddeuci, W. S. Broecker, D. L. Thurber, *Earth Planet. Sci. Lett.* **3**, 338 (1967); W. I. Rose and T. J. Bornhorst, in *Uranium in Volcanic and Volcaniclastic Rocks*, P. C. Goodell and A. C. Waters, Eds. (American Association of Petroleum Geologists Studies in Geology, no. 13, Tulsa, OK, 1981), pp. 13–21; S. Newman, J. D. Macdougall, R. C. Finkel, *Contrib. Mineral. Petrol.* **93**, 195 (1986).
64. A. Zindler and S. R. Hart, *Annu. Rev. Earth Planet. Sci.* **14**, 493 (1986).
65. A. W. Hofmann, *Earth Planet. Sci. Lett.* **90**, 297 (1988).
66. E. Widom and J. Gill, abstract of paper presented at the International Association of Volcanology and Chemistry of the Earth's Interior, Mainz, Germany, 1990.
67. O. Sigmarsson, M. Condomines, E. Ibarrola, *J. Volcanol. Geotherm. Res.*, in press.
68. Ch. Hemond *et al.*, *Earth Planet. Sci. Lett.* **87**, 273 (1988); O. Sigmarsson, M. Condomines, S. Fourcade, *ibid.* **110**, 149 (1992).
69. H. Keppler and P. J. Wyllie, *Contrib. Mineral. Petrol.* **109**, 139 (1991); J. M. Brennan and E. B. Watson, *Earth Planet. Sci. Lett.* **107**, 672 (1991).
70. The half-life of ^{10}Be is 1.5×10^6 years. This isotope is abundant in young pelagic sediment but absent from young volcanic rocks except at subduction zones where the ^{10}Be is introduced to the source by the subduction of young sediment. [J. D. Morris, *Annu. Rev. Earth Sci.* **19**, 313, (1991)]. Consequently, the numerators in element and isotope ratios that are positively correlated with ^{10}Be/^{9}Be are likely to be slab derived [J. D. Morris, W. P. Leeman, F. Tera, *Nature* **334**, 31 (1990)].
71. M. Condomines and O. Sigmarsson, in preparation.
72. J. D. Macdougall and G. Lugmair, *Earth Planet. Sci. Lett.* **77**, 273 (1986); J. Eaby, D. A. Clague, J. R. Delaney, *J. Geophys. Res.* **89**, 7883 (1984); A. S. Davis and D. A. Clague, *ibid.* **92**, 10,467 (1987); B. Dupré, B. Lambret, D. Rousseau, C. J. Allègre, *Nature* **294**, 552 (1981); Ch. Hemond, thesis, Université Paris VII (1986); M. McCulloch and M. Perfit, *Earth Planet. Sci. Lett.* **56**, 167 (1981); W. White and J. Patchett, *ibid.* **67**, 167 (1984); D. J. Whitford, *Geochim. Cosmochim. Acta* **39**, 1287 (1975); A. N. Halliday *et al.*, *Earth Planet. Sci. Lett.* **63**, 241 (1983); M. Cortini, *Bull. Volcanol.* **44**, 711 (1982); ——— and O. Hermes, *Contrib. Mineral. Petrol.* **77**, 44 (1981).
73. We thank our former students R. Williams, O. Sigmarsson, M. Reagan, and E. Widom for discussion of these topics. Supported by a NATO grant for joint work between our research groups.